Compositional disorder and its influence on the structural, electronic, and magnetic properties of $MgC(Ni_{1-x}Co_x)_3$ alloys from first principles

P. Jiji Thomas Joseph and Prabhakar P. Singh
Department of Physics, Indian Institute of Technology Bombay, Mumbai 400076, India
(Received 23 August 2005; revised manuscript received 23 October 2005; published 14 December 2005)

First-principles, density-functional based electronic structure calculations are carried out for $MgC(Ni_{1-x}Co_x)_3$ alloys over the concentration range $0 \leqslant x \leqslant 1$, using Korringa-Kohn-Rostoker coherent-potential approximation method in the atomic sphere approximation. The self-consistent calculations are used to study the changes as a function of x in the equation of state parameters, total and partial densities of states, magnetic moment and the on-site exchange interaction parameter. To study the magnetic properties as well as its volume dependence, fixed-spin moment calculations in conjunction with the phenomenological Landau theory are employed. The salient features that emerge from these calculations are (i) a concentration independent variation in the lattice parameter and bulk modulus at $x \sim 0.75$ with an anomaly in the variation of the pressure derivative of bulk modulus, (ii) the fixed-spin moment based corrections to the overestimated magnetic ground state for $0.0 \leqslant x \leqslant 0.3$ alloys, making the results consistent with the experiments, and (iii) the possibility of multiple magnetic states at $x \sim 0.75$, which, however, requires further improvements in the calculations.

DOI: 10.1103/PhysRevB.72.214206 PACS number(s): 71.20.Be, 74.25.Jb, 71.15.Nc

I. INTRODUCTION

Much of the interest in the 8 K cubic perovskite superconductor $MgCNi_3$ (Ref. 1) stems from its spectral distribution of electronic states.[2–7] A sharp peak, primarily composed of Ni $3d$ bands show up in the density of states spectra, suggesting that the material is close to a ferromagnetic instability.[2,3] Theoretical calculations based on the Stoner model as well as the NMR experiments reveal the possibility of coexistence of spin fluctuation with superconductivity.[3,8] This makes $MgCNi_3$ a material in a class of its own, since according to conventional models of superconductivity magnetic scattering is thought to induce pair-breaking effects. A simple case study is that of the binary cubic VN alloy in which the expected superconducting transition temperature is about 30 K, which is lowered down to ~6 K due to spin fluctuations.[9,10]

The origin of the incipient magnetism in $MgCNi_3$ could be partly attributed to the presence of C in its octahedral interstitial position.[11] The spatially extended C $2p$ orbitals strongly hybridize with that of the Ni $3d$, delocalizing the electronic states. As a result the density of states at the Fermi energy $N(E_F)$ falls short of satisfying the Stoner criteria. It is suggested that approximately 0.5 holes, which may correspond to 10% of Mg replaced by an alkali metal, or about 7% replacement of Ni with Co, would drive the corresponding material magnetic.[2,3,5] The latter follows the rigid-band model, where the Fermi level is expected to lower in energy with respect to hole concentration, thus making E_F coincide with the transition-metal-derived $3d$ singularity.

Previously, studies of hole dopings via vacancies and B substitutions in the C sublattice[12] and Fe and Co substitutions in the Ni sublattice have been carried out.[13–22] In none of the above cases, a definite magnetic solution was found feasible. For Co substitutions the experimental results are unambiguous over the fact that T_C decreases as Co at. % increases in the disordered $MgC(Ni_{1-x}Co_x)_3$ alloys.[13,15,17,18] However, they remain controversial on the rate at which the T_C is decreased.[17,18] Resistivity characterization shows that T_C decreases gradually with increasing x. A small superconducting transition is observed for the samples with $x=0.5$, which indicates that the superconducting volume fraction decreases upon substitution of Co for Ni.[18] However, this is inconsistent with the susceptibility measurements where Co in dilute limit is found to completely suppress the superconductivity, although no magnetic long-range order is detected.[16] The rapid loss of superconductivity is argued to be consistent with magnetic quenching of the superconductivity, probably in the form of spin fluctuations.

Co forms a complete solid solution in $MgCNi_3$ in the cubic perovskite structure. In $MgC(Ni_{1-x}Co_x)_3$ alloys, the ferromagnetic onset is estimated to be around 0.75 at. % of Co.[17] Further, experiments as well as theoretical calculations suggest that a complete replacement of Ni with Co drive in a definite ferromagnetic ground state.[13–15] The Co local moment in $MgCCo_3$ is calculated to be $0.33\mu_B$ with the magnetization energy being equal to 22 mRy.[14,15] Theoretical calculations also reveal that the stoichiometrically ordered alloys $MgCNi_2Co$ and $MgCNiCo_2$ remain nonmagnetic.[14,15]

As a precursor to understanding the nature of magnetic instability in $MgCNi_3$, a theoretical study of Co substitution in the Ni sublattice was carried out. To study the effects of compositional disorder on the structural, electronic and magnetic properties of $MgC(Ni_{1-x}Co_x)_3$ alloys we have employed the Green's function technique in conjunction with the coherent-potential approximation.[23,24] The versatility of the method allows a relative comparison of the alloy energetics of the stoichiometrically ordered alloys and their disordered counterparts.

In the present work, we have studied the changes in the equation of state parameters, density of states and the magnetic properties as a function of x in $MgC(Ni_{1-x}Co_x)_3$ alloys.

Both self-consistent as well as the fixed-spin moment method[25] in conjunction with the phenomenological Landau theory of phase transition are employed to study the magnetic properties of the disordered $MgC(Ni_{1-x}Co_x)_3$ alloys.

The paper is organized as follows. In Sec. II, we briefly describe the computational details. Section III contains the results and discussion in terms of equation of state parameters, electronic structure and magnetic properties of $MgC(Ni_{1-x}Co_x)_3$ alloys.

II. COMPUTATIONAL DETAILS

The ground state properties are calculated using the Korringa-Kohn-Rostoker (KKR) method formulated in the atomic-sphere approximation (ASA).[23,24] Chemical disorder in the Ni sublattice with Co, are assumed to be completely random and is accounted for by means of coherent-potential approximation (CPA).[26] For improving the alloy energetics, the ASA is corrected by the use of both the muffin-tin correction for the Madelung energy[27] and the multipole moment correction to the Madelung potential and energy.[28,29] These corrections bring significant improvements in the calculations by taking into account the nonspherical part of the polarization effects.[30] Note that the electrostatic interactions are obviously a key contribution to the effective interactions between differently charged cations.

The partial waves in the KKR-ASA calculations are expanded up to $l_{\max}=3$ inside the atomic spheres. The multipole moments of the electron density have been determined up to $l^M_{\max}=6$, and then used for the multipole moment correction to the Madelung energy. The exchange-correlation effects are taken into consideration via the local-density approximation (LDA) with Perdew and Wang parametrization.[31] The core states have been recalculated after each iteration. The calculations are partially scalar relativistic in the sense that although the wave functions are nonrelativistic, first order perturbation corrections to the energy eigenvalues due to the Darwin and the mass-velocity terms are included. Further, screening constants α and β were incorporated in the calculations, following the prescription of Ruban and Skriver.[28] These values were estimated from the order(N) locally self-consistent Green's function method[32] and were determined to be 0.83 and 1.18, respectively. The atomic sphere radii of Mg, C, and Ni/Co were kept as 1.404, 0.747, and 0.849 of the Wigner-Seitz radius, respectively. The overlap volume of the atomic spheres was less than 15%, which is legitimate within the accuracy of the approximation.[33] The total energies were calculated with 1771 **k** points in the irreducible wedge of the Brillouin zone. The convergence in charge density was achieved so that the root-mean square of moments of the occupied partial density of states becomes smaller than 10^{-6}.

Numerical calculations of magnetic energy $\Delta E(M)$ for $MgC(Ni_{1-x}Co_x)_3$ alloys were carried out at their self-consistently determined equilibrium lattice constants using the fixed-spin moment method of alloy theory.[25] In the fixed-spin moment method the total energy is obtained for a given magnetization M, i.e., by fixing the numbers of electrons with up and down spins. In this case, the Fermi energies in the up and down spin bands are not equal to each other because the equilibrium condition would not be satisfied for arbitrary M. At the equilibrium M two Fermi energies will coincide with each other. The total magnetic energy becomes minimum or maximum at this value of M.

The diffraction experiments measure displacements as large as 0.05 for the Ni atoms in $MgCNi_3$. These, however are found to be less significant towards any qualitative analysis of the materials properties. The first-principles calculations ignoring these effects, thereby assuming a rigid perfect underlying cubic symmetry, find no profound magnetic effects emerging, unlike in the case of Fe impurities in fcc Al or in bcc Zr.[34–37,40,41] Although in disordered alloys lattice relaxations around an impurity is important, for 3d impurities in a 3d host these effects seem to be less important.[37–39] Usually, such effects stem from large atomic size mismatch of the host and the impurity atoms which is, however, not the case for Co and Ni ions.

III. RESULTS AND DISCUSSION

The $MgC(Ni_{1-x}Co_x)_3$ alloys are theoretically characterized in terms of the variation of physical properties as a function of x. These include the equation of state parameters such as lattice constant, bulk modulus and its pressure derivative, electronic structure expressed in terms of total, sublattice resolved partial and l-decomposed density of states. The magnetic properties are determined via both the self-consistent calculations and the fixed-spin moment calculations, including the variation in the Co local moment and the on-site exchange interaction constant as a function of x. For $x<0.3$, the self-consistent calculations yield ambiguous results about the magnetic ground state of $MgC(Ni_{1-x}Co_x)_3$ alloys, therefore, we used the fixed-spin moment method in this concentration range. These calculations find that for low Co rich alloys, the ground state is definitely paramagnetic. In conjunction with the Landau theory the $MgC(Ni_{1-x}Co_x)_3$ alloys for $0.0\leqslant x\leqslant 0.3$ show a greater propensity of magnetism. However, both the self-consistent as well as the fixed-spin moment calculations yield consistent results for $x\geqslant 0.75$ alloys.

A. Equation of state parameters

The equilibrium lattice constants of $MgC(Ni_{1-x}Co_x)_3$ alloys for $0\leqslant x\leqslant 1$ were determined by calculating the total energy at six lattice constants close to the expected equilibrium lattice constant and then using the third-order Birch-Murnaghan equation of state.[42,43] Since the choice of the exchange correlation term in the Kohn-Sham Hamiltonian is crucial in determining the equation of state parameters we have carried out the calculations using three different exchange correlation functionals namely the local density approximation (LDA), the generalized gradient approximation (GGA),[44] and the local Airy gas (LAG) approximation.[45] One may note that the Birch-Murnaghan equation is derived from the theory of finite strain, by considering an elastic isotropic medium under isothermal compression, with the assumption that the pressure-volume relation remains linear.

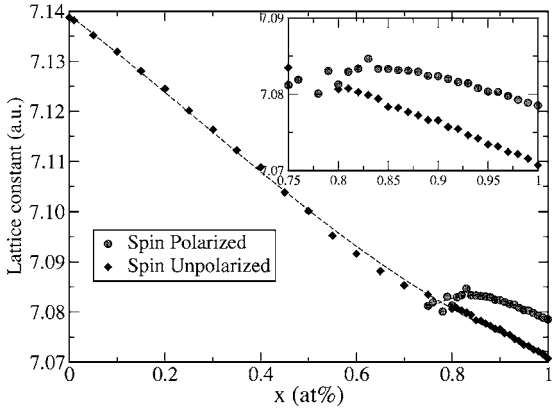

FIG. 1. The variation in the lattice constant of $MgC(Ni_{1-x}Co_x)_3$ as a function of x calculated using the KKR-ASA-CPA method. Results for both spin polarized and unpolarized calculations are shown.

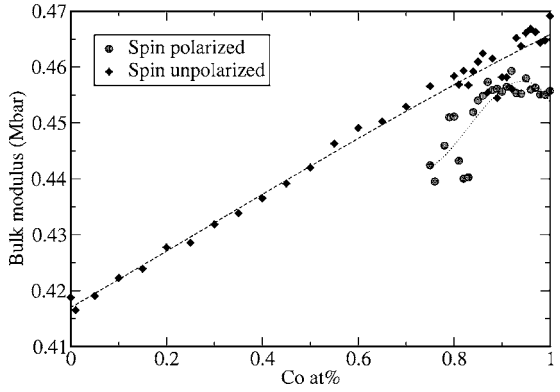

FIG. 2. The variation in the bulk modulus for $MgC(Ni_{1-x}Co_x)_3$ alloys as a function of x, calculated using the KKR-ASA-CPA method. Results for both spin polarized and unpolarized calculations are shown.

The polynomial would yield a reasonable guess to the equation of state parameters provided the fit is chosen in a volume range close to equilibrium.

The equilibrium lattice constants for $MgC(Ni_{1-x}Co_x)_3$ alloys decrease as x increases. This is consistent with the fact that the ionic radii of Co is less than that of Ni. For $MgCNi_3$ the equilibrium lattice constant was calculated to be 7.139, 7.305, and 7.233 a.u., in the LDA, GGA, and LAG approximations, respectively. When compared to the experiments, we find that LDA underestimates the value of the lattice constant by 1%, while both GGA and LAG overestimate the value. The LDA estimate matches well with the previous full-potential report of Singh and Mazin.[3] We note that the consistency with the full-potential methods is because of the muffin-tin correction to the ASA, without which the KKR-ASA calculations find the equilibrium lattice constant for $MgCNi_3$ as 6.986 a.u. For $MgCCo_3$, the equilibrium lattice constants for both spin polarized and unpolarized calculations turn out to be 7.078 and 7.071 a.u, respectively. A small increase in the lattice constant in the spin polarized calculations is consistent with the fact that magnetization through exchange splitting requires larger volume.

The variation of the lattice constants as a function of x in $MgC(Ni_{1-x}Co_x)_3$ alloys, following both spin unpolarized and polarized calculations is shown in Fig. 1. The salient features that emerge are (i) deviation from the Vegard's law, (ii) a weak x dependence of the lattice constant in the range $0.7 \leqslant x \leqslant 0.8$, and (iii) deviation of lattice constants above $x=0.7$. Deviation from the Vegard's law suggests a diversity in the interatomic interactions. The Vegard's law implicitly assumes that the chemical constituents which make up the alloy have similar potentials and that their distribution remains truly random. Although one may assume Co and Ni to have similar features, the nature of interactions in them is significantly different because $MgCNi_3$ is paramagnetic while $MgCCo_3$ is ferromagnetic. This indicates that the $C\ 2p$ hybridization with the transition metal $3d$ bands in $MgCNi_3$ and $MgCCo_3$ are different and that the Ni-C hybridization would be stronger than the Co-C counterpart in $MgCCo_3$.

The insensitivity of the lattice constant of $MgC(Ni_{1-x}Co_x)_3$ alloys with respect to x in the range $0.7 < x < 0.8$ arises due to a balance between the chemical binding forces and the magnetic ones. Chemical binding tends to compress the lattice while magnetization via exchange splitting of bands requires large volume. These two opposing forces set in to provide an invariance in the lattice constant for $0.7 < x < 0.8$ in $MgC(Ni_{1-x}Co_x)_3$ alloys. For $x > 0.7$, the spin polarized calculations yield slightly higher lattice constants compared to the spin unpolarized calculations, which is purely due to the magnetic effects.

The bulk modulus is proportional to the second derivative of the energy-volume curve. The LDA usually underestimates the lattice constant thus leading to an overestimation of bulk modulus. The emphasis here, however, is to make a qualitative judgment about the bulk modulus as a function of x. Figure 2 shows the change in the isothermal bulk modulus of $MgC(Ni_{1-x}Co_x)_3$ alloys as a function of x for $0 \leqslant x \leqslant 1$. We find that the bulk modulus increases with increasing x.

Assuming that the alloys are isotropic and that the Debye approximation holds, the bulk modulus scales in proportion to the Debye temperature $\Theta_D (\propto B_0^{1/2})$. Higher the value of Θ_D higher the lattice stiffness. In $MgCNi_3$ the frequency of a soft acoustic Ni-based phonon mode calculated in the harmonic approximation tends to become negative.[46,47] Stabilization of this mode results in a dynamic displacement of the Ni ions perpendicular to the Ni-C direction which then allows each of the Ni atoms to move away from the neighboring C atoms towards the empty interstitial. Partial replacement of Ni with Co weakens the bonding with the C atoms. This reduces the advantage of relaxations or distortions thereby increasing Θ_D, thus a concurrent hardening of the phonon modes. When compared to the spin unpolarized calculations, the spin polarized ones yield a lower bulk modulus, which is directly correlated with their corresponding lattice constants.

Since the pressure derivatives of the bulk modulus involves higher order derivatives, they are often noisy. Qualitatively, however, in the Debye approximation the pressure derivatives of the bulk modulus contain the information of the averaged lattice vibrations of the material via the Gruneissen parameter. If one assumes that all the vibrational modes respond to volume in a similar fashion, then they are often useful in interpreting the structural details of the mate-

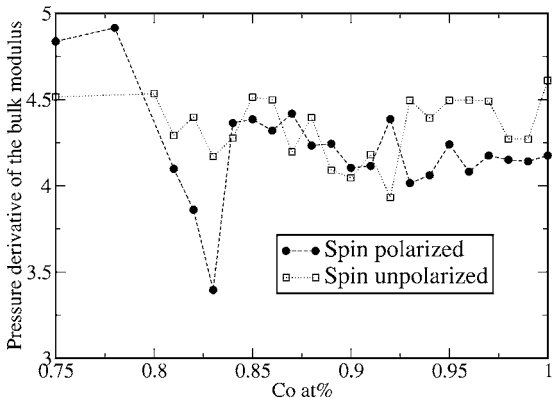

FIG. 3. The change in the pressure derivative of bulk modulus of $MgC(Ni_{1-x}Co_x)_3$ as a function of x calculated using the KKR-ASA-CPA method. Results for both spin polarized and unpolarized calculations are shown.

rial. The variation in the pressure derivative of the bulk modulus, as shown in Fig. 3, suggests an anomaly at $x=0.82$. The discontinuity in the case of spin polarized results suggests that the anomaly could be related to magnetic effects because it appears in the proximity of magnetic onset in the $MgC(Ni_{1-x}Co_x)_3$ alloys.

The versatility of the KKR-ASA method is that it allows a direct comparison of the structural energies of both disordered and ordered alloys. Two ordered alloys can be identified in the concentration range $0<x<1$. These are $MgCNi_2Co$ and $MgCNiCo_2$, which correspond to $x=0.33$ and 0.66, respectively, in the case of disordered $MgC(Ni_{1-x}Co_x)_3$ alloys. Either of these alloys falls in the $0.3<x<0.7$ range, where both spin polarized and unpolarized calculations for the disordered alloys yield degenerate total energies. Table I compares the KKR-ASA structural energies for the ordered and disordered alloys, calculated using three different exchange correlation functionals to Kohn-Sham Hamiltonian. Evidently, from Table I, it follows that for $x=\frac{1}{3}$ the ordered phases are more stable than their disordered counterparts. However, as x increases to $\frac{2}{3}$, the disordered alloys become more stable. The changes in the structural energies provide some clues about the chemical ordering of atoms due to magnetic effects. We plan to report the results in a future work.

The change in the equation of state parameters upon chemical ordering was also calculated using the KKR-ASA

TABLE I. Comparison of the equilibrium total energy expressed in Ry units for $x=\frac{1}{3}$ and $x=\frac{2}{3}$ alloys of $MgC(Ni_{1-x}Co_x)_3$ in three different approximations to V_{xc}; LDA, GGA, and LAG and their difference ($\Delta E=E_{ordered}-E_{disordered}$).

	LDA (Ry)	GGA (Ry)	LAG (Ry)
$MgCNi_2Co$	−1866.120100	−1866.883569	−1869.423046
$MgC(Ni_{0.66}Co_{0.33})_3$	−1866.118525	−1866.882022	−1869.421520
ΔE(mRy)	1.575	1.547	1.526
$MgCNiCo_2$	−1815.219322	−1815.974307	−1818.477701
$MgC(Ni_{0.33}Co_{0.66})_3$	−1815.219848	−1815.974861	−1818.478283
ΔE(mRy)	−0.526	−0.554	−0.573

TABLE II. Comparison of the equation of state parameters for stoichiometrically ordered and disordered alloys using the LDA-KKR-ASA- CPA method.

	a_{eq}(a.u.)	B_{eq}(Mbar)	B'_{eq}
$MgCNi_2Co$	7.113	0.432	4.325
$MgC(Ni_{0.66}Co_{0.33})_3$	7.114	0.433	4.326
$MgCNiCo_2$	7.086	0.451	4.463
$MgC(Ni_{0.33}Co_{0.66})_3$	7.088	0.451	4.237

method in conjunction with the Birch-Murnaghan equation of state with LDA. The results are shown in Table II. The calculations show that the disordered alloys have slightly higher lattice constant than their stoichiometrically ordered counterparts.

B. Electronic structure

Electronic structure of $MgC(Ni_{1-x}Co_x)_3$ alloys are characterized both by means of spin unpolarized and polarized density of states, calculated using the KKR-ASA-CPA method. For $x<0.75$, spin unpolarized density of states are shown while for $x>0.75$, both spin unpolarized and polarized density of states are shown.

1. Spin unpolarised density of states

In Fig. 4, we show the total and sublattice resolved density of states of $MgCNi_3$ and $MgCCo_3$ calculated at their equilibrium lattice constants. The isolated deep valence states in Fig. 4 are essentially the C 2*s* states. Further higher in energy, a gap opens up followed by an admixture of C 2*p* and metal 3*d* states. The strong hybridization is manifested in the DOS as a wide energy spread of the C 2*p* and the transition metal 3*d* states. From Fig. 4 it follows that the hybridization between the C-Ni orbitals are stronger than the C-Co orbitals in their respective alloys. Hybridization gives

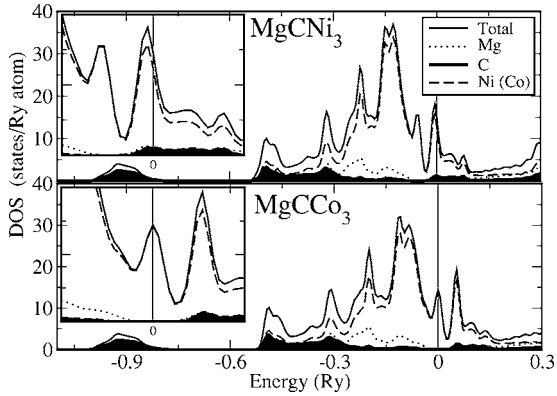

FIG. 4. The spin unpolarized total and sublattice resolved partial density of states for $MgCNi_3$ (upper panel) and $MgCCo_3$ (lower panel) calculated at their equilibrium lattice constants. In the inset, a blow up around the Fermi energy for the corresponding alloys are shown. The vertical line through energy zero represents the alloy Fermi energy.

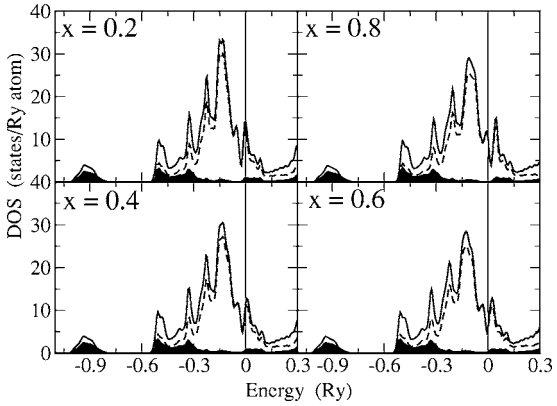

FIG. 5. The spin unpolarized total (solid line), sublattice resolved C (shaded), and $(Ni_{1-x}Co_x)_3$ density of states, with x as shown in the panels, for $MgC(Ni_{1-x}Co_x)_3$ alloys. The vertical line through energy zero corresponds to the alloy Fermi energy.

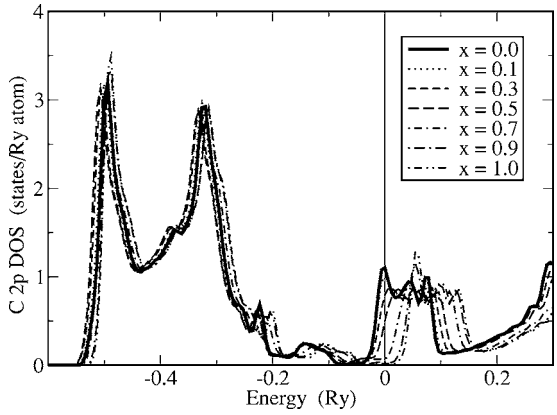

FIG. 6. The spin unpolarized sublattice resolved C $2p$ DOS for $MgC(Ni_{1-x}Co_x)_3$ with x as shown in the panel. The vertical line through energy zero corresponds to the alloy Fermi energy.

not only an important mixing between the states of the conduction bands but also leads to a separation of the bonding and antibonding states, creating a pseudogap. Existence of pseudogaps have been reported in various crystalline solids, amorphous alloys[48] and also in quasicrystals.[49,50] Of the two mechanisms, ionic and covalent, proposed for the formation of pseudogap in alloys the latter is found to play a significant role in the case of transition-metal-based intermetallics. The pseudogap in hexagonal close-packed transition metal rich systems are largely attributed to metal d resonance. Though the Mg-Ni(Co) bonding is weak, a peak just below −0.4 Ry constitutes the bonding between $3s$ electrons of Mg and the transition metal $3d$ electrons in their respective alloys. The striking difference in the DOS of $MgCNi_3$ and $MgCCo_3$ is the absence of C $2p$ states at the E_F for $MgCCo_3$. In $MgCCo_3$ the $N(E_F)$ is entirely due to the CO $3d$ states while for $MgCNi_3$ the C $2p$ contribution to $N(E_F)$ is about 7%.

The present KKR-ASA-CPA calculations find $N(E_F)$ for $MgCNi_3$ to be 14.56 state/Ry atom. The value is, however, at variance with the previous reports. For example, Szajek reports the value as 14.32 state/Ry atom,[51] Mazin and Singh report as 13.57 states/Ry atom,[3] Shim *et al.* as 14.52 states/Ry atom,[4] Rosner *et al.* as 13.06 states/Ry atom.[2] Dugdale and Jarlborg[5] report $N(E_F)$ to be 17.27 and 9.49 states/Ry atom[5] for two different band-structure methods with exchange-correlation effects considered in the LDA and using the experimental lattice constant. These results show that $N(E_F)$ is indeed sensitive to the type of the electronic structure method employed and also to the numerical values of the parameters similar to those of the Wigner-Seitz radii and others. Note that these differences are significant as they control the proximity to magnetism in the Stoner model, as emphasized by Singh and Mazin.[3] For $MgCCo_3$ the value of $N(E_F)$ is determined to be 14.43 state/Ry atom, in agreement with the earlier reports.

Figure 5 shows the spin unpolarized, total and sublattice resolved partial DOS for $MgC(Ni_{1-x}Co_x)_3$ alloys for $x=0.2$, 0.4, 0.6, and 0.8. The overall characteristic features of the DOS structure are preserved as x increases in $MgC(Ni_{1-x}Co_x)_3$, however, with the sharp structures being smeared out due to disorder. As x increases, the decreasing electron count is followed by the inward movement of E_F on the energy scale. The bottom of the states, however, remain more or less fixed with respect to the alloy E_F as a function of x. At about $x=0.7$ the E_F is pinned in the pseudogap. The resulting $N(E_F)$ is minimum for these alloys over the whole concentration profile. As x increases further from 0.7, the $N(E_F)$ gradually increases due to the Co $3d$ states. A high $N(E_F)$, predominantly metal $3d$ in character, thus increases the possibility of exchange splitting of bands in $MgC(Ni_{1-x}Co_x)_3$.

One may note that the C $2p$ states in and around E_F decrease with increasing x, and virtually cease to exist for $x>0.7$ alloys. Since the number of C electrons remains invariant, one may then naturally expect a significant charge redistribution on the energy scale. This is illustrated in Fig. 6. Though the overall shape of the DOS remains the same, a significant charge redistribution over the energy range −0.6 to −0.2 Ry is observed.

In Fig. 7, we show the evolution of the states at E_F as a function of x in $MgC(Ni_{1-x}Co_x)_3$ alloys. Initially with increase in x, the $N(E_F)$ slightly increases, however, not as expected from the rigid band model of alloy theory. Disorder

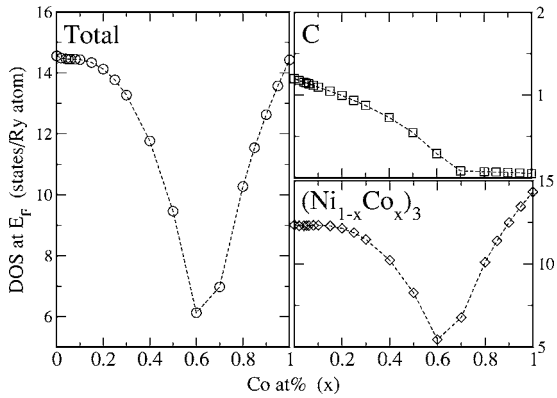

FIG. 7. The variation in the total density of states at Fermi energy as a function of x in $MgC(Ni_{1-x}Co_x)_3$ for $0 \leqslant x \leqslant 1$ alloys in units of states/Ry cell.

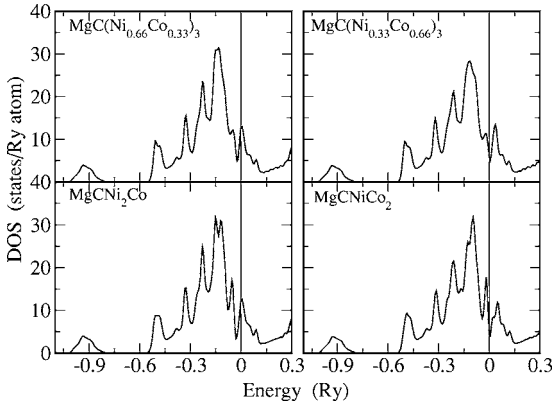

FIG. 8. A comparison of the spin unpolarized total DOS of stoichiometrically ordered and disordered $MgC(Ni_{1-x}Co_x)_3$ alloys for $x=\frac{1}{3}$ and $\frac{2}{3}$, respectively. The vertical line represents the Fermi energy.

smears out the Ni 3*d*-derived van Hove peak of $MgCNi_3$ considerably.

Thus the essential difference between the DOS of $MgCNi_3$ and $MgCCo_3$ is the absence of C contribution to $N(E_F)$. One can find that for both $MgCNi_3$ and $MgCCo_3$ the $N(E_F)$ are comparable and are equal to 14.557 and 14.425 states/Ry atom, respectively. However, their properties are found to be significantly different. $MgCNi_3$ is nonmagnetic with incipient magnetism akin to spin-fluctuations being anticipated, while $MgCCo_3$ is a nonsuperconductor with a definite ferromagnetic state.

The change in the total density of states for the chemically ordered $MgCNi_2Co$ and $MgCNiCo_2$ alloys with respect to their disordered counterparts, $MgC(Ni_{0.66}Co_{0.33})_3$ and $MgC(Ni_{0.33}Co_{0.66})_3$, respectively, are shown in Fig. 8. The overall characteristic features of the DOS remain essentially the same, with exception to the peak broadening in the disordered alloys. The change in the Ni 3*d* and Co 3*d* states for the corresponding ordered and disordered alloys are shown in Fig. 9 and the change in the C partial DOS is shown in Fig. 10.

2. Spin polarized density of states

With $N(E_F)$ in the paramagnetic DOS showing high values for $x>0.75$ and with no C 2*p* states at or near E_F, a possibility of electronic distortion leading to a ferromagnetic ground state can well be anticipated. Taking the cue, spin polarized calculations were carried out for $MgC(Ni_{1-x}Co_x)_3$ alloys for $0.7 \leqslant x \leqslant 1.0$.

Figure 11 shows the spin polarized, total and sublattice resolved partial DOS of $MgCCo_3$. The deep states are primarily C 2*s* states. Higher in energy and close to E_F, the states are predominately Co 3*d* in character. As expected, the Co 3*d* bands are exchange split due to magnetic effects. As a measure of the exchange splitting on the energy scale, we find the difference between the centres of the 3*d* up bands $C_B^{\uparrow}$ and that of the down bands $C_B^{\downarrow}$ as 22 mRy, which corresponds to a local magnetic moment of $0.33\mu_B$. These values are consistent with earlier full-potential calculations. Small exchange splitting of the Mg and *C* 2*p* bands are seen due to

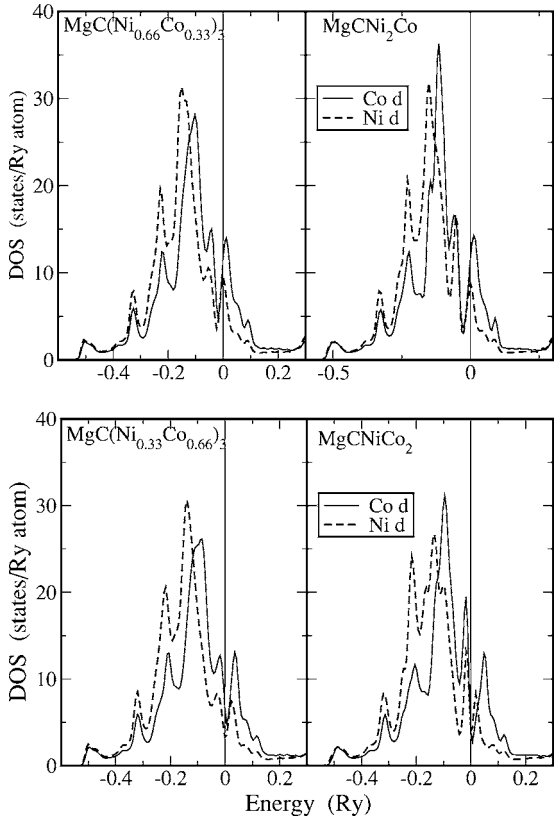

FIG. 9. A comparison of spin unpolarized, sublattice resolved transition metal DOS of stoichiometrically ordered and disordered $MgC(Ni_{1-x}Co_x)_3$ alloys for $x=\frac{1}{3}$ (upper panel) and $\frac{2}{3}$ (lower panel). The vertical line represents the Fermi energy.

hybridization effects, however, the splittings are negligible when compared to that of the Co 3*d* bands.

The changes in the DOS as a function of *x* in $MgC(Ni_{1-x}Co_x)_3$ alloys are shown in Fig. 12. For both majority and minority bands, the deep states essentially consist of *C* 2*s* states. Higher in energy towards E_F, a gap opens up followed by an admixture of *C* 2*p* metal 3*d* states. The spin up bands are fully occupied and the E_F for these states are

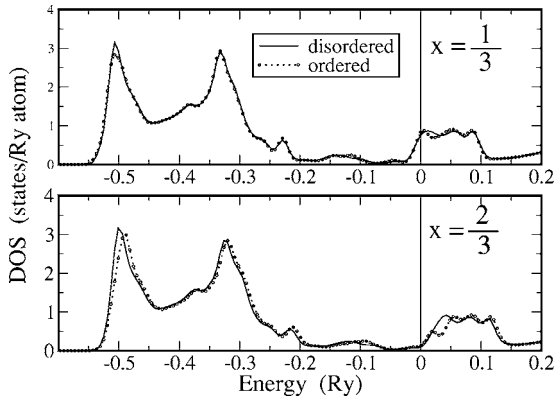

FIG. 10. A comparison of spin unpolarized sublattice resolved partial *C* 2*p* DOS of stoichiometrically ordered and disordered $MgC(Ni_{1-x}Co_x)_3$ alloys for $x=\frac{1}{3}$ (upper panel) and $\frac{2}{3}$ (lower panel). The vertical line represents the Fermi energy.

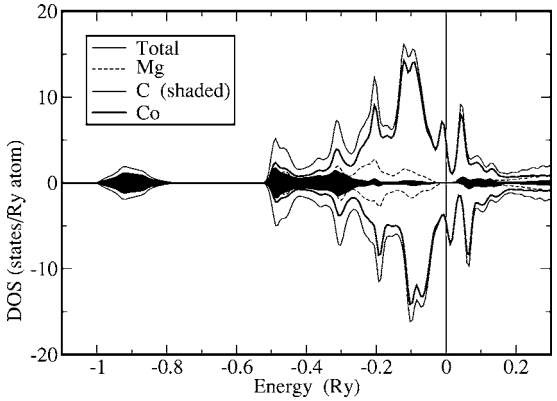

FIG. 11. The spin polarized total and sub-lattice resolved partial spin up and down DOS of $MgCCo_3$. The vertical line through the energy zero represents the Fermi energy and + and − DOS represent the majority and minority spin DOS respectively.

pinned in the pseudogap. For the spin down states, the E_F moves slightly inward with increasing x. Magnetism is thus governed by the change in the position of E_F in the minority DOS with respect to that of the majority bands.

The sublattice resolved, concentration weighted, l-decomposed $3d$ DOS of $MgC(Ni_{1-x}Co_x)_3$ alloys are as shown in Fig. 13, where the exchange splitting as well as the distortions can be seen clearly. It also becomes evident that not all d substates are equally exchange split. Relatively, d_{yz} and d_{3z^2-1} bands show the maximum exchange splitting, while the states contained in the x-y plane, the distortions in the majority and minority bands are more noticeable. Distortions result due to significant charge transfer. Bonding is anisotropic due to covalent character along the x-y plane and rather metallic character along the z direction.

C. Magnetic properties

1. Variation of Co local moment

In general, when a paramagnetic DOS shows a high $N(E_F)$, with E_F in the antibonding region, the system is close

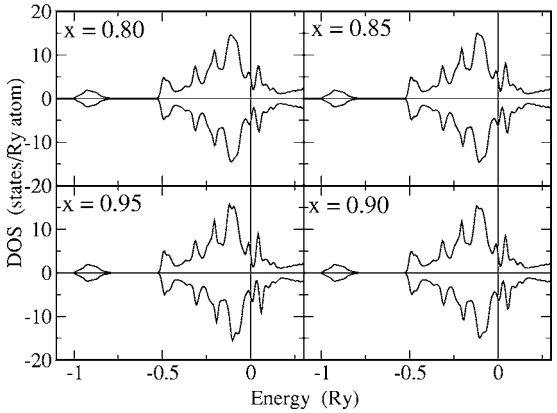

FIG. 12. The spin polarized total density of states of $MgC(Ni_{1-x}Co_x)_3$ alloys for $0.85 \leqslant x \leqslant 0.95$. The vertical line through the energy zero represents the Fermi energy and + and − DOS represent the majority and minority spin DOS respectively.

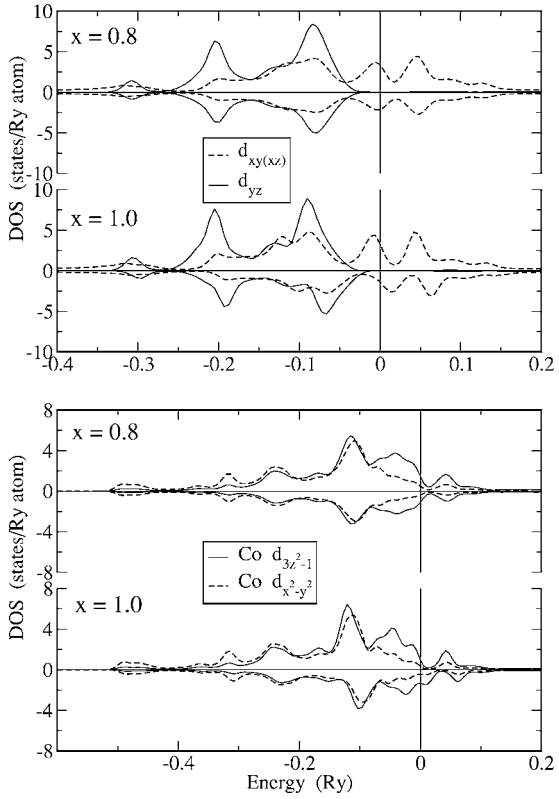

FIG. 13. The spin polarized, sublattice resolved and orbital decomposed *Co* $3d$ partial density of states for $0.85 \leqslant x \leqslant 0.95$ alloys. The vertical line through the energy zero represents the Fermi energy.

to a magnetic instability. Under these conditions, distortion inevitably decreases the total energy. The first choice, however, is a reshuffling of the electronic states instead of the atoms getting displaced. The electrons prefer to rearrange themselves resulting in a spontaneous magnetization thereby lowering the electronic symmetry and annihilating the antibonding states.

According to Dronskowski *et al.*,[52,53] antiferromagnetism is likely to step in when the paramagnetic DOS has E_F in a nonbonding region. For those systems, where E_F is in the antibonding region, exchange splitting of bands towards ferromagnetism is more likely. In $MgCNi_3$ the E_F is in the antibonding region, and hence it is closer to ferromagnetic instability rather than an antiferromagnetic one. Further, antiferromagnetism had been ruled out in $MgCNi_3$ owing to the absence of nesting features in the Fermi surface topology.

The present calculations find small moments at the Co site for $x \leqslant 0.3$, as shown in Fig. 14. The results are inconsistent with experiments. Some of the factors that can influence the magnetic moment at the Co site are the choice of the sphere radii, inadequate basis set used to expand the wave functions, lack of lattice relaxation and local environment effects. In this direction, calculations were carried out for different sphere radii, but the local moment at the Co site remained inevitable. To include local environment effects, supercell calculations based on the LMTO-ASA as well as locally self consistent Green's function method were employed, however, the Co remained magnetic. Since common to all the

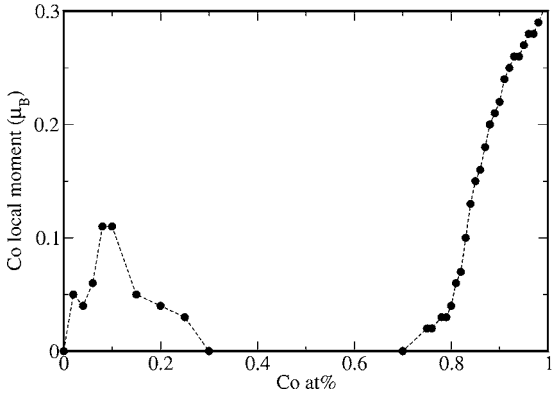

FIG. 14. The variation in the Co local magnetic moment in $MgC(Ni_{1-x}Co_x)_3$ alloys calculated using the KKR-ASA- CPA method in LDA for $0 \leqslant x \leqslant 1$.

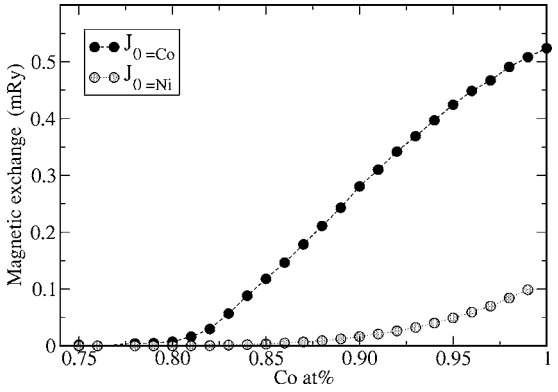

FIG. 15. The variation of the on-site exchange coupling constant J_0 in mRy, as a function of $x > 0.75$ in $MgC(Ni_{1-x}Co_x)_3$ alloys.

above calculations was LDA, the appearance of local magnetic moment at *Co* site was thought to be due to the limitations of LDA itself.

It is known that first-principles LDA based calculations for materials such as FeAl,[54] Ni_3Ga,[55] $Sr_3Ru_2O_7$,[56] $SrRhO_3$,[57] and $Na_{0.5}CoO_2$ (Refs. 58 and 59) yield a finite local moment in disagreement with the experiments which find them to be paramagnetic. The error that evolved due to LDA in the present self-consistent calculations for $MgC(Ni_{1-x}Co_x)_3$ alloys, was, however, corrected by means of the fixed-spin moment method, the results of which we show below.

2. On-site magnetic exchange interactions

The total exchange coupling parameter J_0 is calculated as a function of $x, x > 0.7$ following the prescription of Liechtenstein *et al.*[60] Essentially the method is based on mapping the change in energy due to the deviation of a single spin at a reference site "*o*," from the collinear ferromagnetic ground state onto an effective Heisenberg model. The change in the energy corresponding to this small spin density perturbation is approximated by the change in the sum of one electron energies by appealing to Andersen's local force theorem. Using Lloyd's formula one can express the sum of one electron energies in terms of scattering path operator or the auxiliary Green's function. The latter can be evaluated from the knowledge of potential functions and the structure constant matrix. Mapping the change in energy onto a Heisenberg model results in an expression for the exchange coupling constant

$$J_0 = \sum_i J_{0i}$$

which is the sum of exchange interactions between the reference spin and all its neighbors. In a mean field theory this coupling constant is proportional to the Curie temperature T_C of the system. For a multicomponent random alloy the mean field estimate of the T_C can be assumed to be the concentration-weighted average of the coupling constants calculated for the component atoms. Thus, for the case of $MgC(Ni_{1-x}Co_x)_3$ alloys, the average coupling constant can be calculated as

$$J_0 \equiv (1-x)J_{\mathrm{Ni}} + (x)J_{\mathrm{Co}},$$

where J_i (i=Ni or Co) is given as

$$J_i = -\frac{1}{4\pi}\sum_L \int^{E_F} dE\, \mathrm{Im}\{\Delta_L^i(z)[T_{L\uparrow}^i(z) - T_{L\downarrow}^i(z)] + \Delta_L^i(z)T_{L\uparrow}^i(z)\Delta_L^i(z)T_{L\downarrow}^i(z)\}$$

with

$$\Delta_L^i = P_{L\uparrow}^i(z) - P_{L\downarrow}^i(z),$$

$$P_{L\sigma}^i(z) = [z - C_{L\sigma}^i][\Delta_{L\sigma}^i + \gamma_{L\sigma}^j(z - C_{L\sigma}^i)]^{-1},$$

$$T_{L\sigma}^i(z) = \langle g_{L\sigma}(z)\rangle\{1 + (P_{L\sigma}(z) - \tilde{P}_{L\sigma}(z))\langle g_{L\sigma}(z)\rangle\},$$

where σ is the spin index ($\uparrow$ or $\downarrow$), and $P_{L\sigma}^i$ is the potential function of the component i for the orbital L and spin σ. The potential function has been expressed above in terms of C, Δ, and γ of the LMTO Hamiltonian, z is the complex energy and E_F is the Fermi energy of the alloy, $\langle g_{L\sigma}(z)\rangle$ is the configurationally averaged auxiliary Green's function within CPA and $\tilde{P}_{L\sigma}(z)$ is the coherent-potential of the medium. The CPA calculations are performed by invoking site-site approximation.

Figure 15 shows the variation in the J_{Ni} and J_{Co} as a function of x in $MgC(Ni_{1-x}Co_x)_3$ alloys. Both J_{Co} and μ_{Co} (Fig. 14) follow a similar trend. Both show a slow variation in and around the ferromagnetic onset followed by a sharp increase, further getting saturated when $x \to 1$. Except for an overestimation of the exchange coupling constant, the calculations are expected to produce the correct trend. The disappearance of the average Co local moment is accompanied by disappearance of the average exchange interaction J_{Co}, a result which can be related to the strong magnetovolume effect.

3. Fixed-spin moment calculations

The density functional theory is an exact ground state theory. However, common approximations similar to the

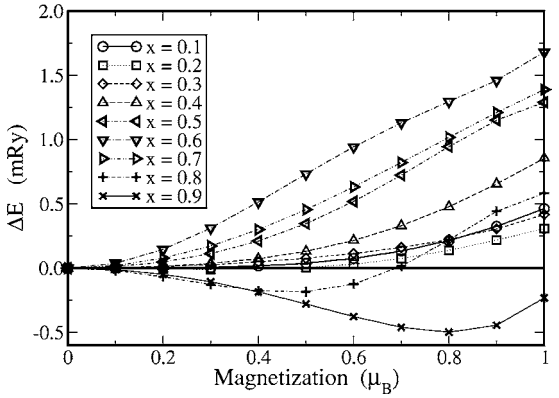

FIG. 16. The variation in the $\Delta E(M)$ as a function of magnetization M, calculated at the respective equilibrium volume for $MgC(Ni_{1-x}Co_x)_3$ alloys as a function of x, as indicated in the figure.

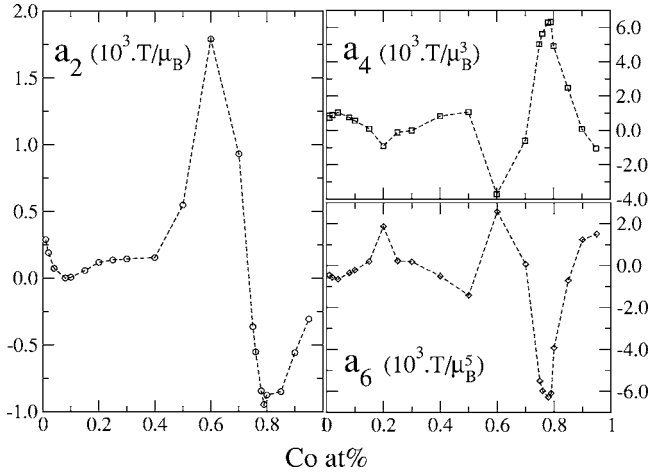

FIG. 17. The variation of Ginzburg-Landau coefficients as a function of *Co* concentration (x) in $MgC(Ni_{1-x}Co_x)_3$ alloys.

LDA to the density functional theory is thought to miss certain important physics due to the assumption of a uniform electron gas especially when spin-fluctuation effects are important. The effects of spin-fluctuations are, however, described on a phenomenological level using the Ginzburg-Landau theory. Although a robust quantitative theory based on first-principles is yet to be implemented, it is possible to make an estimate of spin-fluctuation effects based on LDA fixed-spin moment calculations.

According to Mazin and others,[61] the overestimation of the tendency of metals towards ferromagnetism within the LDA can be used as an indicator of critical fluctuations in a material. However, for this to be an effective indicator, competing states, such as anti-ferromagnetism need to be ruled out in each material. As mentioned above, since E_F resides in the antibonding region as well as the absence of nesting features in the Fermi surface topology of $MgCNi_3$ shows that the material under consideration may be far from any antiferromagnetic instability.

For $MgC(Ni_{1-x}Co_x)_3$, the overestimation of the moments for $x<0.3$ could be taken as an indication of spinfluctuations, following the works of Singh and Mazin.[3] However, no attempt is made to determine the magnitude of the fluctuations in the present work. The study is limited to understanding the propensity of magnetism with Co substitutions, for which one can use the phenomenological Ginzburg-Landau coefficients, the input to which follows from the fixed-spin moment method.

Numerical calculations of magnetic energy $\Delta E(M)$ for $MgC(Ni_{1-x}Co_x)_3$ alloys in the range $0 \leqslant x \leqslant 1$ are carried out by the fixed-spin moment method. One can then write down a Ginzburg-Landau expansion for the magnetic energy $\Delta E(M)=\Sigma_{i\geqslant 1}^{n}(1/2i)a_{2i}M^{2i}$ for $n=3$. The variation of $\Delta E(M)$ with respect to M is shown in Fig. 16. For $x \leqslant 0.3$, the curves are relatively flat near $M=0$ and fit well to the form as given above with $n=3$. The sensitivity of $\Delta E(M)$ with M becomes more distinguishable as x increases from 0.3 and beyond, i.e., the flatness of the curve disappears. For $x>0.7$ the magnetic energy is negative, indicating a lower energy ferromagnetic state to be stable.

Figure 17 shows the variation of Ginzburg-Landau coefficients a_2 and a_4 as a function of x in $MgC(Ni_{1-x}Co_x)_3$ alloys. The coefficient a_2 is of prime importance and is used as a precursor to indicate the magnetic phase of the system. A positive a_2 represents the paramagnetic state while a negative a_2 indicates the ferromagnetic state. From Fig. 17 we find that initially, as x increases, a_2 tends to zero, but remains positive. This indicates that a ferromagnetic state is unstable for low Co rich alloys. However for $x>0.75$, a_2 is negative indicating a ferromagnetic state for the system. These calculated results are now consistent with the experiments, which show a definite paramagnetic phase for low Co rich alloys and a magnetic state for high Co rich alloys.

As the unit cell volume is increased, E_F is lowered in energy. This will then sharpen the structures in the DOS. If $N(E_F)$ then satisfies the Stoner criterion, i.e., $IN(E_F)>1$, where I is the Stoner exchange integral, then the system would become magnetic. Having seen that the self-consistent calculations yield ambiguous magnetic properties, one can extend the fixed-spin moment calculations to the magnetization dependence of $MgC(Ni_{1-x}Co_x)_3$ with respect to the unit cell volume.

Figure 18 shows the variation of the magnetic energy as a function of volume, expressed in terms of its equilibrium volume V_0, for $x=0.01$, 0.1 and 0.2, respectively. For $x=0.01$, an expansion by 8% shows no magnetic phase for the alloy. However, for both $x=0.1$ as well as $x=0.2$, a magnetic phase looks possible just above its equilibrium volume. The curves dip into the negative region of the magnetic energy as can be seen from the middle and the bottom panel of Fig. 18, respectively, where the ferromagnetic state is lower in energy.

For $x=0.1$ and 0.2, a ferromagnetic phase becomes stable just above its equilibrium volume suggesting a magnetovolume instability in $MgC(Ni_{1-x}Co_x)_3$ alloys. Fitting the above data to the Ginzburg-Landau expression for $n=3$ for the three concentrations $x=0.01$, 0.10, and 0.20, one finds that for expanded volumes a magnetic phase becomes definitely possible as Co at. % increases in $MgC(Ni_{1-x}Co_x)_3$.

Figure 19 shows the variation of the Ginzburg-Landau coefficients as a function of volume ratio for $x=0.01$, 0.10, and 0.20, respectively. For V/V_0 slightly greater than unity,

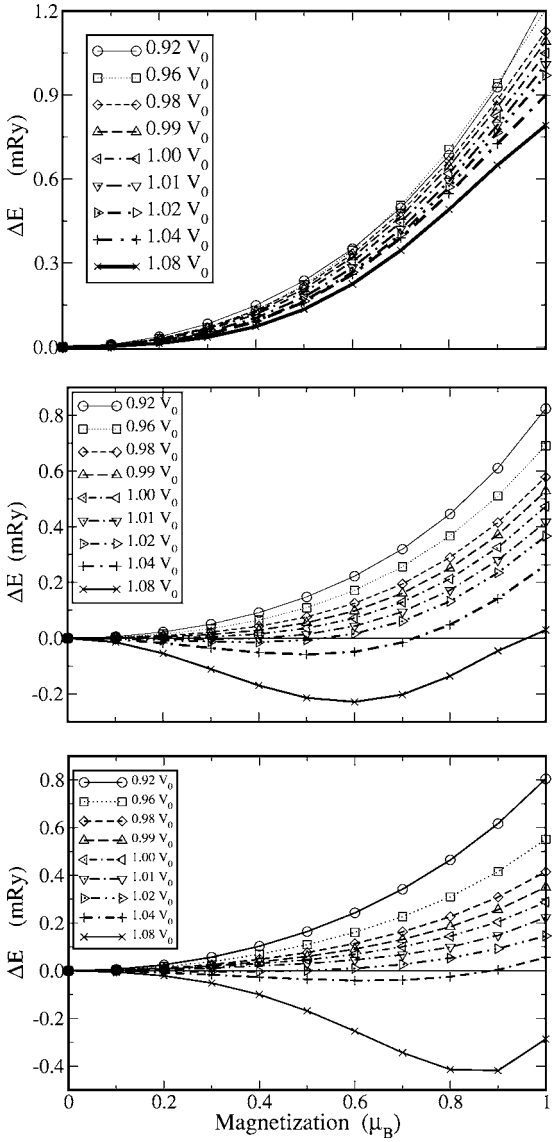

FIG. 18. The variation of $\Delta E(M)$ as a function of M for $MgC(Ni_{1-x}Co_x)_3$ alloys at various volume ratios as indicated in the fig. for (a) $x=0.01$ (upper panel), (b) $x=0.1$ (middle panel), and (c) $x=0.2$ (lower panel).

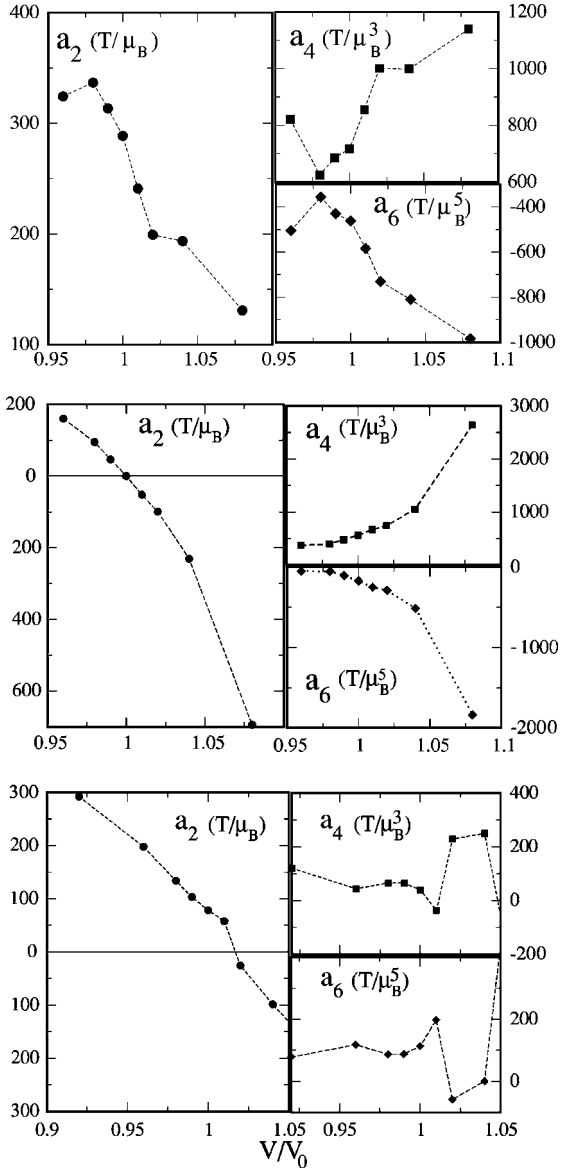

FIG. 19. The variation of the Ginzburg-Landau coefficients a_2 (in units of T/μ_B), a_4 (in units of $\frac{T}{\mu_B^3}$), and a_6 (in units of T/μ_B^5) as a function of volume for $MgC(Ni_{1-x}Co_x)_3$ alloys for (a) $x=0.01$ (upper panel), (b) $x=0.1$ (middle panel), and (c) $x=0.2$ (lower panel).

for both $x=0.1$ and $x=0.2$, the coefficient a_2 reverses its sign, indicating a phase transition with respect to volume. This confirms that these alloys are on the verge of a magnetovolume instability. The higher order coefficients play a significant role in determining the alloy magnetic properties.

It has also been noted that the accuracy of the total energy, evaluated by means of ASA is limited to a few mRy. From calculations, one finds that the change in the energy is far too small for any reliable quantitative analysis. However, within the approximations mentioned and with well defined **k** mesh in the Brillouin zone, one can certainly infer that the trend produced via the fixed-spin moment method for $MgC(Ni_{1-x}Co_x)_3$ alloys are qualitatively correct.

IV. CONCLUSIONS

For low Co-rich $MgC(Ni_{1-x}Co_x)_3$ alloys, we find the possibility of enhanced spinfluctuations in the material, which is close to a ferromagnetic instability. However, for Co-rich alloys, a definite ferromagnetic ground state exists. At the magnetic crossover, i.e., for $x=0.75$, a concentration independent variation in the structural properties are determined. For example, the lattice constant and the bulk modulus appear to be constant under the given approximations of the KKR-ASA-CPA theory. The pressure derivative of the bulk modulus indicates, within the Debye approximation, a significant change in the averaged vibrational modes. Our calculations show that the electronic structure of the disordered $MgC(Ni_{1-x}Co_x)_3$ alloys deviates significantly from that of the rigid band model. The striking feature is the recession of C $2p$ states towards lower energies as a function of increasing x in $MgC(Ni_{1-x}Co_x)_3$ alloys. The self-consistent calculations

overestimate the magnetic moments at the Co site for low Co rich alloys, due to the limitations in the local-density approximation. Corrections to the overestimation in the magnetic moments are accomplished by means of fixed-spin moment method, in conjunction with the Ginzburg-Landau free energy functional. It then follows from the fixed-spin moment calculations that for $x<0.7$ the material is definitely paramagnetic.

[1] T. He, K. A. Regan, M. A. Hayward, A. P. Ramirez, Y. Wang, P. Khalifah, T. He, J. S. Slusky, N. Rogado, K. Inumaru, M. K. Haas, H. W. Zandbergen, N. P. Ong, and R. J. Cava, Nature (London) **411**, 54 (2001)

[2] H. Rosner, R. Weht, M. D. Johannes, W. E. Pickett, and E. Tosatti, Phys. Rev. Lett. **88**, 027001 (2002)

[3] D. J. Singh and I. I. Mazin, Phys. Rev. B **64**, 140507(R) (2001)

[4] J. H. Shim, S. K. Kwon, and B. I. Min, Phys. Rev. B **64**, 180510(R) (2001)

[5] S. B. Dugdale and T. Jarlborg, Phys. Rev. B **64**, 100508(R) (2001)

[6] I. G. Kim, J. I. Lee, and A. J. Freeman, Phys. Rev. B **66**, 174512 (2002)

[7] J. H. Kim, J. S. Ahn, J. Kim, Min-Seok Park, S. I. Lee, E. J. Choi, and S.-J. Oh, Phys. Rev. B **66**, 172507 (2002)

[8] P. M. Singer, T. Imai, T. He, M. A. Hayward, and R. J. Cava, Phys. Rev. Lett. **87**, 257601 (2001)

[9] H. Rietschel, H. Winter, and W. Reichardt, Phys. Rev. B **22**, 4284 (1980)

[10] H. Rietschel, Phys. Rev. B **24**, 155 (1981)

[11] P. J. T. Joseph and P. P. Singh, cond-mat/0504659 (unpublished).

[12] T. Klimczuk, M. Avdeev, J. D. Jorgensen, R. J. Cava, cond-mat/0412551 (unpublished).

[13] I. R. Shein, A. L. Ivanovskii, E. Z. Kurmaev, A. Moewes, S. Chiuzbian, L. D. Finkelstein, M. Neumann, Z. A. Ren, and G. C. Che Phys. Rev. B **66**, 024520 (2002).

[14] J. L. Wang, Y. Xu, Z. Zeng, Q. Q. Zheng, and H. Q. Lin, J. Appl. Phys. **91**, 8504 (2002).

[15] I. G. Kim, J. I. Lee, and A. J. Freeman, Phys. Rev. B **65**, 064525 (2002).

[16] M. A. Hayward, M. K. Haas, A. P. Ramirez, T. He, K. A. Regan, N. Rogado, K. Inumaru, and R. J. Cava, Solid State Commun. **119**, 491 (2001)

[17] Z. A. Ren, G. C. Che, S. L. Jia, H. Chen, Y. M. Ni, and Z. X. Zhao, cond-mat/0105366 (unpublished).

[18] T. G. Kumary, J. Janaki, A. Mani, S. M. Jaya, V. S. Sastry, Y. Hariharan, T. S. Radhakrishnan, and M. C. Valsakumar, Phys. Rev. B **66**, 064510 (2002).

[19] F. M. Liu, J. Q. Li, C. Dong, T. M. Wang, Y. Q. Zhou, and H. Chen, Semicond. Sci. Technol. **15**, 1316 (2002).

[20] A. Das and R. K. Kremer, Phys. Rev. B **68**, 064503 (2003).

[21] M. Alzamora, D. R. Sanchez, M. Cindra, and E. M. Baggio-Saitovitch, Braz. J. Phys. **32**, 755 (2002)

[22] M. S. Park, J. S. Gim, S. H. Park, Y. W. Lee, S. I. Lee, and E. J. Choi, Semicond. Sci. Technol. **17**, 274 (2004).

[23] J. S. Faulkner, Prog. Mater. Sci. **27**, 1 (1982)

[24] I. Turek, V. Drchal, J. Kudrnovsky, M. Sob, and P. Weinberger, *Electronic Structure of Disordered Alloys, Surfaces and Interfaces* (Kluwer Academic, Dordrecht, 1997).

[25] K Schwarz and P. Mohn, J. Phys. F: Met. Phys. **14**, L129 (1984).

[26] P. Soven, Phys. Rev. **156**, 809 (1967).

[27] N. E. Christensen and S. Satpathy, Phys. Rev. Lett. **55**, 600 (1985).

[28] A. V. Ruban and H. L. Skriver, Phys. Rev. B **66**, 024201 (2002).

[29] A. V. Ruban, S. I. Simak, P. A. Korzhavyi, and H. L. Skriver, Phys. Rev. B **66**, 024202 (2002).

[30] A. V. Ruban and H. L. Skriver, Comput. Mater. Sci. **15**, 119 (1999).

[31] J. P. Perdew and Y. Wang, Phys. Rev. B **45**, 13244 (1992).

[32] I. A. Abrikosov, S. I. Simak, B. Johansson, A. V. Ruban, and H. L. Skriver Phys. Rev. B **56**, 9319 (1997)

[33] H. L. Skriver, *The LMTO method, Muffin Tin Orbitals and Electronic Structure* (Springer-Verlag, Berlin, 1984).

[34] F. Lechermann, M. Fahnle, B. Meyer, and C. Elsasser, Phys. Rev. B **69**, 165116 (2004).

[35] P. G. Gonzales, L. A. Terrazos, H. M. Petrilli, and S. Frota-Pessoa, Phys. Rev. B **57**, 7004 (1998).

[36] D. Guenzburger and D. E. Ellis, Phys. Rev. Lett. **67**, 3832 (1991).

[37] N. Papanikolaou, R. Zeller, P. H. Dederichs, and N. Stefanou, Comput. Mater. Sci. **8**, 131 (1997).

[38] N. Papanikolaou, R. Zeller, P. H. Dederichs, and N. Stefanou, Phys. Rev. B **55**, 4157 (1997).

[39] B. Drittler, M. Weinert, R. Zeller, and P. H. Dederichs, Phys. Rev. B **39**, 930 (1989).

[40] S. Frota-Pessoa, L. A. de Mello, H. M. Petrilli, and A. B. Klautau, Phys. Rev. Lett. **71**, 4206 (1993).

[41] A. Metz, S. Frota-Pessoa, J. Kapoor, D. Riegel, W. D. Brewer, and R. Zeller, Phys. Rev. Lett. **71**, 3525 (1993).

[42] F. Birch, J. Geophys. Res. **57**, 227 (1952).

[43] F. D. Murnaghan, *Finite Deformation of an Elastic Solid* (Wiley, New York, 1951), p. 140.

[44] J. P. Perdew, K. Burke, and Y. Wang, Phys. Rev. B **54**, 16 533 (1996).

[45] L. Vitos, B. Johansson, J. Kollar, and H. L. Skriver, Phys. Rev. B **62**, 10 046 (2000).

[46] A. Yu. Ignatov, S. Y. Savrasov, and T. A. Tyson, Phys. Rev. B **68**, 220504(R) (2003).

[47] R. Heid, B. Renker, H. Schober, P. Adelmann, D. Ernst, and K.-P. Bohnen, Phys. Rev. B **69**, 092511 (2004)

[48] Didier Mayou and Alain Pasturel, J. Phys.: Condens. Matter **1**, 9685 (1989).

[49] M. Krajci, J. Hafner, and M. Mihalkovic, Europhys. Lett. **34**, 207 (1996).

[50] H. Matsubara, S. Ogawa, T. Kinoshita, K. Kishi, S. Takeuchi, K. Kimura1, and S. Suga, Jpn. J. Appl. Phys., Part 2 **30**, L389 (1991)

[51] A. Szajek, J. Phys.: Condens. Matter **13**, L595 (2001).

[52] R. Dronskowski, Int. J. Quantum Chem. **96**, 89 (2003).

[53] A. Decker, G. A. Landrum, and R. Dronskowski, Z. Anorg. Allg. Chem. **628**, 303 (2002).

[54] A. G. Petukhov I. I. Mazin, L. Chioncel, and A. I. Lichtenstein, Phys. Rev. B **67**, 153106 (2003).

[55] A. Aguayo, I. I. Mazin, and D. J. Singh, Phys. Rev. Lett. **92**, 147201 (2004).
[56] D. J. Singh and I. I. Mazin, Phys. Rev. B **63**, 165101 (2001).
[57] D. J. Singh, Phys. Rev. B **67**, 054507 (2003).
[58] D. J. Singh, Phys. Rev. B **61**, 13 397 (2000).
[59] D. J. Singh, Phys. Rev. B **68**, 020503(R) (2003).
[60] A. I. Liechtenstein, M. I. Katsnelson, and V. A. Gubanov, J. Phys. F: Met. Phys. **14**, L125 (1984)
[61] I. I. Mazin, D. J. Singh, and A. Aguayo, in *Proceedings of the NATO ARW on Physics of Spin in Solids: Materials, Methods and Applications*, edited by S. Halilov (Kluwer, Dordrecht, 2003).